Neural Networks 22 (2009) 949–957

Contents lists available at ScienceDirect

Neural Networks

journal homepage: www.elsevier.com/locate/neunet

Optimal exponential synchronization of general chaotic delayed neural networks: An LMI approach ☆

Meiqin Liu *

Department of Systems Science and Engineering, College of Electrical Engineering, Zhejiang University, Hangzhou 310027, PR China

ARTICLE INFO

Article history:
Received 11 December 2007
Received in revised form 3 October 2008
Accepted 15 April 2009

Keywords:
Exponential synchronization
Optimal control
Drive–response conception
Lyapunov–Krasovskii functional
Linear matrix inequality
Generalized eigenvalue problem (GEVP)
Chaotic neural network
Time-delay feedback control

ABSTRACT

This paper investigates the optimal exponential synchronization problem of general chaotic neural networks with or without time delays by virtue of Lyapunov–Krasovskii stability theory and the linear matrix inequality (LMI) technique. This general model, which is the interconnection of a linear delayed dynamic system and a bounded static nonlinear operator, covers several well-known neural networks, such as Hopfield neural networks, cellular neural networks (CNNs), bidirectional associative memory (BAM) networks, and recurrent multilayer perceptrons (RMLPs) with or without delays. Using the drive–response concept, time-delay feedback controllers are designed to synchronize two identical chaotic neural networks as quickly as possible. The control design equations are shown to be a generalized eigenvalue problem (GEVP) which can be easily solved by various convex optimization algorithms to determine the optimal control law and the optimal exponential synchronization rate. Detailed comparisons with existing results are made and numerical simulations are carried out to demonstrate the effectiveness of the established synchronization laws.

1. Introduction

Since Aihara firstly introduced chaotic neural network model to simulate the chaotic behavior of biological neurons (Aihara, Takabe, & Toyoda, 1990), chaotic neural networks have been successfully applied in combinational optimization (Kwok & Smith, 2000), associative memory (Tan & Ali, 2001), secure communication (Milanovic & Zaghloul, 1996), chemical biology (Han, Kurrer, & Kuramoto, 1995), and so on. At present, there are two methods to construct chaotic neural networks. First, the networks are connected by a number of chaotic neurons or chaotic oscillators in the same way as Hopfield networks (Aihara et al., 1990; Milanovic & Zaghloul, 1996), such as Hindmarsh–Rose neurons (Yu & Peng, 2006), etc. Second, some dynamic neural network with special connected weights can exhibit chaotic behaviors, such as Hopfield neural networks (Cheng, Liao, & Hwang, 2005), cellular neural networks (CNNs) (Lu & Leeuwen, 2006), bidirectional associative memory (BAM) networks (Bueno & Araujo, 2006), recurrent multilayer perceptrons (RMLPs), etc. Research on the synchronization of chaotic neural networks has broadened considerably in the last few years. Synchronization in chaotic systems has found many applications. It was used to understand self-organization behavior in the brain as well as in ecological systems, and it has been applied to secure communications (Lu & Leeuwen, 2006). A wide variety of approaches have been proposed for the synchronization and control of the above chaotic neural networks with or without delays which include linear and nonlinear feedback control, adaptive design control, the impulsive control method, and the invariant manifold method, among many others (see Bueno and Araujo (2006), Chen and Dong (1998), Cheng et al. (2005), Fradkov and Evans (2005), He, Cao, Zhu, and Ogura (2003), He and Cao (2008), Li, Fei, Zhu, and Cong (2008), Lu and Leeuwen (2006), Lu and Cao (2007), Sun and Cao (2007), Tang, Qiu, Fang, Miao, and Xia (2008) and Zhou, Chen, and Xiang (2006) and the references cited therein).

However, to our best knowledge, the aforementioned methods and many other existing synchronization methods give the existing conditions of controllers, and hardly provide the solution algorithms of the controller parameters. On the other hand, there does not seem to be much (if any) study on the optimal exponential synchronization and its optimal convergence rate for chaotic neural networks based on the linear matrix inequality (LMI) approach. It is well known that there are many stability criteria given on the basis of LMI for dynamic neural networks (Liao, Chen, & Sanchez, 2002a, 2002b; Liu, 2006; Wang & Cao, 2006), since the LMI approach has the advantage that it can be solved numerically and very effectively using for instance

☆ This work was supported in part by the National Natural Science Foundation of China under Grant 60504024 and 60874050, in part by the Research Project of Zhejiang Provincial Education Department under Grant 20050905, in part by the Zhejiang Provincial Natural Science Foundation of China under Grant Y106010, and in part by the Specialized Research Fund for the Doctoral Program of Higher Education (SRFDP), China under Grant 20060335022. This work was also supported by the "151 Talent Project" of Zhejiang Province (No. 05-3-1013 and No. 06-2-034).

* Tel.: +86 571 87951313; fax: +86 571 87951313.
E-mail addresses: liumeiqin@zju.edu.cn, mliu2@uno.edu.

0893-6080/$ – see front matter © 2009 Elsevier Ltd. All rights reserved.
doi:10.1016/j.neunet.2009.04.002

the interior-point method (Boyd, Ghaoui, Feron, & Balakrishnan, 1994; Nesterov & Nemirovsky, 1994) or computing software (Gahinet, Nemirovsky, Laub, & Chilali, 1995). Therefore, here we will combine the LMI approach and the Lyapunov–Krasovskii functional to investigate the optimal synchronization problem of chaotic neural networks. Distinct from previous investigations, the current study focuses on the synthesis of an optimal exponential synchronization controller, and the solvability of the optimal synchronization problem for chaotic neural networks with or without time delays. The main advantages of the present approach include: (i) it not only provides a design procedure of synchronization controller such that the synchronization errors exponentially converge to zeros in designated rates, but also obtains an optimal controller by solving the LMI standard problem (i.e. generalized eigenvalue problem) according to the requirement of performance, or implementation in practice; (ii) it is less conservative and less restrictive than the ones given in Cheng et al. (2005) and Lu and Leeuwen (2006), and easy to derive synchronization conditions in LMI form.

For second type of chaotic neural networks, many researchers have studied their synchronization or control problem based on the common neural network model in Cheng et al. (2005), Lu and Leeuwen (2006), Lu and Cao (2007), Sun and Cao (2007), Sun, Cao, and Wang (2007) and Zhou et al. (2006). However, although this common model can unify several neural networks such as Hopfield neural networks (Yang & Yuan, 2005), CNNs (Cheng et al., 2005; Lu & Leeuwen, 2006), and BAM neural networks (Bueno & Araujo, 2006), it does not describe neural networks composed of multi-layer structure such as RMLPs (Barabanov & Prokhorov, 2002) or including time-varying parameters such as Cohen–Grossberg neural networks (CGNNs) (Cohen & Grossberg, 1983). Here, we are inspired by the standard neural network model (SNNM) in Liu (2006) and put forward a general chaotic neural network, which is the interconnection of a linear delayed dynamic system and a bounded static nonlinear operator. Most chaotic systems with (or without) time delays can be transformed into this general chaotic neural network to be synchronization synthesized in a unified way.

The rest of this paper is organized as follows. In Section 2, the general chaotic neural network model considered in this paper is presented, and the exponential synchronization problem of the drive–response general chaotic neural networks is then defined. Our main results and the realization of exponential synchronization are described in Section 3. In Section 4, some illustrative examples and their simulations are provided to demonstrate the effectiveness of our proposed approaches. Finally, some concluding remarks are given in Section 5.

2. Notation and preliminaries

Throughout this paper, the following notations will be used: $\mathfrak{R}^n$ denotes n-dimensional Euclidean space, $\mathfrak{R}^{n\times m}$ is the set of all $n \times m$ real matrices, I denotes the identity matrix of appropriate order, and $*$ denotes the symmetric parts. $\lambda_M(A)$ and $\lambda_m(A)$ denote the maximal and minimal eigenvalue of a square matrix A, respectively. $\|x\|$ denotes the Euclid norm of the vector x, and $\|A\|$ denotes the induced norm of the matrix A, that is, $\|A\| = \sqrt{\lambda_M(A^TA)}$. The notations $X > Y$ and $X \geq Y$, where X and Y are matrices of same dimensions, mean that the matrix $X - Y$ is positive definite and positive semi-definite, respectively. If $X \in \mathfrak{R}^p$ and $Y \in \mathfrak{R}^q$, $C(X; Y)$ denotes the space of all continuous functions mapping $\mathfrak{R}^p \to \mathfrak{R}^q$.

In this paper, we consider the following chaotic delayed neural network model (Liu, 2006):

$$\begin{cases} \dot{x}(t) = Ax(t) + A_dx(t-\tau) + B_p\phi(\xi(t)), \\ \xi(t) = C_qx(t) + C_{qd}x(t-\tau) + D_p\phi(\xi(t)), \end{cases} \tag{1}$$

with the initial condition function

$$x(t) = \varpi(t), \quad \forall t \in [-\tau, 0],$$

where $x(t) \in \mathfrak{R}^n$ is the state vector associated with the neurons, $A \in \mathfrak{R}^{n\times n}$, $A_d \in \mathfrak{R}^{n\times n}$, $B_p \in \mathfrak{R}^{n\times L}$, $C_q \in \mathfrak{R}^{L\times n}$, $C_{qd} \in \mathfrak{R}^{L\times n}$, and $D_p \in \mathfrak{R}^{L\times L}$ are the corresponding state-space matrices, $\phi \in C(\mathfrak{R}^L; \mathfrak{R}^L)$ is the nonlinear activation function satisfying $\phi(0) = 0$, $\xi \in \mathfrak{R}^L$ is the input vector of ϕ, $\tau > 0$ is the transmission delay, $\varpi(\cdot)$ is the given continuous function on $[-\tau, 0]$, and $L \in \mathfrak{R}$ is the total number of neurons in the hidden layers and output layer of the neural network.

In this paper, we assume that the activation functions in (1) are monotonically non-decreasing and globally Lipschitz. That is, there exist non-negative scalar q_i and positive scalar h_i such that

$$q_i \leq \frac{\phi_i(\alpha) - \phi_i(\beta)}{\alpha - \beta} \leq h_i, \quad i = 1, \ldots, L, \tag{2}$$

for arbitrary $\alpha, \beta \in \mathfrak{R}$.

Remark 1. The chaotic delayed neural network model (1) is formally similar to a Lur'e system, but is different in essence. In all of references about the synchronization of Lur'e systems (Cao, Li, & Ho, 2005; Chen, Lu, & Chen, 2008; Xiang, Li, & Wei, 2007), the forms of the Lur'e systems are

$$\begin{aligned} &\dot{x}(t) = Ax(t) + Bf(Cx(t)), \quad \text{or} \\ &\dot{x}(t) = Ax(t) + A_dx(t-\tau) + Bf(Cx(t)), \end{aligned} \tag{3}$$

where $f(\cdot)$ satisfies a sector condition or a Lipschitz condition. It can clearly be seen that Eq. (3) is a special case of model (1). Moreover, model (1) also unifies several well-known dynamic neural networks with or without delays such as Hopfield neural networks, CNNs, BAM networks, RMLPs, etc. In Section 4, we will illustrate that these neural network models are special examples of (1). On the other hand, the system (1) reduces to a neural network without delays if $\tau = 0$ or $A_d = 0$ and $C_{qd} = 0$.

It has been shown in Gilli (1993) that dynamic neural networks can exhibit some chaotic behaviors. Therefore, if the state-space matrices and the delay parameter τ are suitably chosen, the system (1) will also display a chaotic behavior. So herein we are concerned with the synchronization problem of system (1). Based on the drive–response concept for synchronization of coupled chaotic systems, which was initially proposed by Pecora and Carroll (1990), the corresponding response system of (1) is given in the following form:

$$\begin{cases} \dot{y}(t) = Ay(t) + A_dy(t-\tau) + B_p\phi(\zeta(t)) + u(t), \\ \zeta(t) = C_qy(t) + C_{qd}y(t-\tau) + D_p\phi(\zeta(t)), \end{cases} \tag{4}$$

with the initial condition function

$$y(t) = \sigma(t), \quad \forall t \in [-\tau, 0], \tag{5}$$

where $y(t) \in \mathfrak{R}^n$ is the state vector, $\sigma(\cdot)$ is the given continuous function on $[-\tau, 0]$, and $u(t) \in \mathfrak{R}^n$ is the state feedback control law given to achieve the exponential synchronization between drive–response systems.

In order to investigate the problem of exponential synchronization between systems (1) and (4), we define the synchronization error signal $e(t) = x(t) - y(t)$, where $x(t)$ and $y(t)$ are the state variables of drive system (1) and response system (4), respectively. Therefore, the error dynamical system between (1) and (4) is given as follows:

$$\begin{cases} \dot{e}(t) = Ae(t) + A_de(t-\tau) + B_p\psi(\eta(t)) - u(t), \\ \eta(t) = C_qe(t) + C_{qd}e(t-\tau) + D_p\psi(\eta(t)), \end{cases} \tag{6}$$

where $e(t) \in \Re^n$, and $\eta(t) = \xi(t) - \zeta(t)$, $\psi(\eta(t)) = \phi(\xi(t)) - \phi(\zeta(t)) = \phi(\eta(t) + \zeta(t)) - \phi(\zeta(t))$; therefore $\psi(0) = 0$. Since all the $\phi_i(\cdot)$ are globally Lipschitz, the $\psi_i(\cdot)$ satisfy the sector conditions, i.e., for each $i = 1, \dots, L$,

$$q_i \le \psi_i(\eta_i(t))/\eta_i(t) \le h_i \quad \text{or} \\ [\psi_i(\eta_i(t)) - q_i\eta_i(t)] \cdot [\psi_i(\eta_i(t)) - h_i\eta_i(t)] \le 0. \tag{7}$$

If the state variables of the drive system (1) are used to drive the response system (4), the control input vector with state and time-delay state feedback is designed as follows:

$$u(t) = K_1 e(t) + K_2 e(t-\tau), \tag{8}$$

where $K_1 \in \Re^{n\times n}$ and $K_2 \in \Re^{n\times n}$ are feedback gain parameters to be scheduled. With the control law (8), the error dynamics can be expressed in the following form:

$$\begin{cases} \dot{e}(t) = (A - K_1)e(t) + (A_d - K_2)e(t-\tau) + B_p\psi(\eta(t)), \\ \eta(t) = C_q e(t) + C_{qd}e(t-\tau) + D_p\psi(\eta(t)), \end{cases} \tag{9}$$

Since $\psi(0) = 0$, system (9) admits a trivial solution: $e(t) \equiv 0$.

Remark 2 (*Sun et al., 2007*). It is well known that time delays always influence the dynamic properties of the chaotic delayed neural networks. Hence, in (8), we add the time-delay feedback control $K_2 e(t-\tau)$. As discussed in Liao and Chen (2003) and Wang, Zhong, Tang, Man, and Liu (2001), such a time-delayed feedback term could be employed to tackle more general systems and achieve less conservative analysis results than those results without using the delayed feedback term.

Before stating the main results, we first need the following definition.

Definition 1 (*Cheng et al., 2005*). The drive system (1) and the response system (4) are said to be exponentially synchronized if, for a suitably designed feedback controller, there exist constants $\lambda \ge 1$ and $\gamma > 0$ such that $\|x(t) - y(t)\| \le \lambda\|x(0) - y(0)\| \exp(-\gamma t)$, for any $t \ge 0$. Moreover, the constant γ is defined as the exponential synchronization rate.

In fact, the exponential synchronization problem considered in this paper is to determine the control input $u(t)$ associated with the state feedback to synchronize the two identical chaotic delayed neural networks exponentially with the same system parameters, but different initial conditions. It is clear that, if the trivial solution of the controlled error dynamical system (9) is exponentially stable, then exponential synchronization between the drive system (1) and the response system (4) can be realized.

3. Main results

We have cast the problem of global exponential synchronization as that of stability of the system (9). This means that we can use Lyapunov functionals and estimation techniques similar as in Liu (2007) to develop theoretical conditions for global exponential synchronization. With these, we can provide design rules for the controller feedback gain matrices K_1, K_2, with which exponential synchronization is ensured.

Theorem 1. *If there exist positive definite matrices X and S, diagonal semi-positive definite matrix T, a positive scalar γ, and matrices Y_1 and Y_2 such that the following nonlinear matrix inequality,*

$$G = \begin{bmatrix} G_{11} & G_{12} & G_{13} \\ * & G_{22} & G_{23} \\ * & * & G_{33} \end{bmatrix} < 0, \tag{10}$$

holds, then the drive system (1) and the response system (4) can be synchronized with an exponential synchronization rate of γ. Moreover, the feedback gains are obtained as $K_1 = Y_1X^{-1}$ and $K_2 = Y_2X^{-1}$. The submatrices of G are

$$G_{11} = (AX - Y_1)^{\mathrm{T}} + AX - Y_1 + 2\gamma X + S, \qquad G_{12} = A_dX - Y_2,$$
$$G_{13} = B_pT + XC_q^{\mathrm{T}}(Q + H),$$
$$G_{22} = -\exp(-2\gamma\tau)S, \qquad G_{23} = XC_{qd}^{\mathrm{T}}(Q + H),$$
$$G_{33} = TD_p^{\mathrm{T}}(Q + H) + (Q + H)D_pT - 2T, \quad \text{where}$$
$$Q = \mathrm{diag}(q_1, q_2, \dots, q_L), \qquad H = \mathrm{diag}(h_1, h_2, \dots, h_L).$$

Proof. Pre-and post-multiplying the left-hand side matrix of (10) by $\mathrm{diag}(X^{-1}, X^{-1}, T^{-1})$, (10) is equivalent to the equation given in Box I.

Let $P = X^{-1}$, $\sum = T^{-1}$, and $\Gamma = X^{-1}SX^{-1}$, and consider $K_1 = Y_1X^{-1}$ and $K_2 = Y_2X^{-1}$, we rewrite the equation given in Box I as the equation given in Box II.

For the error dynamical system (9), we define a positive definite Lyapunov–Krasovskii functional as

$$V(e(t)) = \exp(2\gamma t)\mathrm{e}^{\mathrm{T}}(t)Pe(t) + \int_{-\tau}^{0} \exp(2\gamma(t+\theta))\mathrm{e}^{\mathrm{T}}(t+\theta)\Gamma e(t+\theta)\mathrm{d}\theta,$$

where $P = P^T > 0$, $\Gamma = \Gamma^T > 0$, and $\gamma > 0$. The derivative of $V(e(t))$ along the solution of system (9) is

$$\begin{aligned} \frac{\mathrm{d}V(e(t))}{\mathrm{d}t} &= 2\gamma\exp(2\gamma t)\mathrm{e}^{\mathrm{T}}(t)Pe(t) + 2\mathrm{e}^{2\gamma t}\mathrm{e}^{\mathrm{T}}(t)P[(A - K_1)e(t) \\ &\quad + (A_d - K_2)e(t-\tau) + B_p\psi(\eta(t))] + \exp(2\gamma t)\mathrm{e}^{\mathrm{T}}(t)\Gamma e(t) \\ &\quad - \exp(2\gamma(t-\tau))\mathrm{e}^{\mathrm{T}}(t-\tau)\Gamma e(t-\tau) \\ &= \exp(2\gamma t)[\mathrm{e}^{\mathrm{T}}(t)[(A - K_1)^{\mathrm{T}}P + P(A - K_1) + 2\gamma P + \Gamma]e(t) \\ &\quad + \mathrm{e}^{\mathrm{T}}(t)P(A_d - K_2)e(t-\tau) + \mathrm{e}^{\mathrm{T}}(t)PB_p\psi(\eta(t)) \\ &\quad + \mathrm{e}^{\mathrm{T}}(t-\tau)(A_d - K_2)^{\mathrm{T}}Pe(t) \\ &\quad - \exp(-2\gamma\tau)\mathrm{e}^{T}(t-\tau)\Gamma e(t-\tau) + \psi^{\mathrm{T}}(\eta(t))B_p^{\mathrm{T}}Pe(t)] \\ &= \exp(2\gamma t)\begin{bmatrix} e(t) \\ e(t-\tau) \\ \psi(\eta(t)) \end{bmatrix}^T R_0 \begin{bmatrix} e(t) \\ e(t-\tau) \\ \psi(\eta(t)) \end{bmatrix}, \end{aligned}$$

where

$$R_0 = \begin{bmatrix} (A - K_1)^{\mathrm{T}}P + P(A - K_1) + 2\gamma P + \Gamma & P(A_d - K_2) & PB_p \\ (A_d - K_2)^{\mathrm{T}}P & -\exp(-2\gamma\tau)\Gamma & 0 \\ B_p^{\mathrm{T}}P & 0 & 0 \end{bmatrix}.$$

The sector conditions (7) can be rewritten as follows:

$$\psi_i^2(\eta_i(t)) - \psi_i(\eta_i(t))(q_i + h_i)\eta_i(t) + q_ih_i\eta_i^2(t) \le 0.$$

Since $q_ih_i\eta_i^2(t) \ge 0$, we can obtain

$$\psi_i^2(\eta_i(t)) - \psi_i(\eta_i(t))(q_i + h_i)\eta_i(t) \le 0,$$

which is equivalent to

$$\begin{aligned} &2\psi_i^2(\eta_i(t)) - 2\psi_i(\eta_i(t))(q_i + h_i)C_{q,i}e(t) - 2\psi_i(\eta_i(t))(q_i + h_i) \\ &\quad \times C_{qd,i}e(t-\tau) - 2\psi_i(\eta_i(t))(q_i + h_i)D_{p,i}\psi(\eta(t)) \le 0, \end{aligned} \tag{11}$$

where $C_{q,i}$ denotes the ith row of C_q, $C_{qd,i}$ denotes the ith row of C_{qd}, and $D_{p,i}$ denotes the ith row of D_p. We rewrite (11) in matrix notation as follows:

$$\begin{bmatrix} \begin{pmatrix} (X^{-1}A - X^{-1}Y_1X^{-1})^{\mathrm{T}} + X^{-1}A \\ -X^{-1}Y_1X^{-1} + 2\gamma X^{-1} + X^{-1}SX^{-1} \end{pmatrix} & X^{-1}A_d - X^{-1}Y_2X^{-1} & X^{-1}B_p + C_q^{\mathrm{T}}(Q+H)T^{-1} \\ * & -\exp(-2\gamma\tau)X^{-1}SX^{-1} & C_{qd}^{\mathrm{T}}(Q+H)T^{-1} \\ * & * & D_p^{\mathrm{T}}(Q+H)T^{-1} + T^{-1}(Q+H)D_p - 2T^{-1} \end{bmatrix} < 0$$

Box I.

$$\begin{bmatrix} \begin{pmatrix} (PA - PK_1)^{\mathrm{T}} + PA \\ -PK_1 + 2\gamma P + \Gamma \end{pmatrix} & PA_d - PK_2 & PB_p + C_q^{\mathrm{T}}(Q+H)\Sigma \\ * & -\exp(-2\gamma\tau)\Gamma & C_{qd}^{\mathrm{T}}(Q+H)\Sigma \\ * & * & D_p^{\mathrm{T}}(Q+H)\Sigma + \Sigma(Q+H)D_p - 2\Sigma \end{bmatrix} < 0$$

Box II.

$$\begin{bmatrix} e(t) \\ e(t-\tau) \\ \psi_1(\eta_1(t)) \\ \vdots \\ \psi_{i-1}(\eta_{i-1}(t)) \\ \psi_i(\eta_i(t)) \\ \psi_{i+1}(\eta_{i+1}(t)) \\ \vdots \\ \psi_L(\eta_L(t)) \end{bmatrix}^{\mathrm{T}} R_i \begin{bmatrix} e(t) \\ e(t-\tau) \\ \psi_1(\eta_1(t)) \\ \vdots \\ \psi_{i-1}(\eta_{i-1}(t)) \\ \psi_i(\eta_i(t)) \\ \psi_{i+1}(\eta_{i+1}(t)) \\ \vdots \\ \psi_L(\eta_L(t)) \end{bmatrix} \le 0, \tag{12}$$

where R_i is given in Box III, in which $s_i = q_i + h_i$, $d_{p,i,j}$ is the entry of the matrix D_p at the ith row and jth column. By the S-procedure (Boyd et al., 1994) and Box II, if there exist $\varepsilon_i \ge 0$ ($i = 1, \ldots, L$), such that the inequality given in Box IV holds, where $\Sigma = \mathrm{diag}(\varepsilon_1, \varepsilon_2, \ldots, \varepsilon_L)$, and $\Sigma \ge 0$, then $R_0 < 0$; that is, $\mathrm{d}V(e(t))/\mathrm{d}t \le 0$; therefore, $V(e(t)) \le V(e(0))$. However,

$$\begin{aligned} V(e(0)) &= e(0)^{\mathrm{T}}Pe(0) + \int_{-\tau}^{0} \exp(2\gamma\theta)e^{\mathrm{T}}(\theta)\Gamma e(\theta)\mathrm{d}\theta \\ &\le \lambda_M(P)\,\|e(0)\|^2 + \lambda_M(\Gamma)\int_{-\tau}^{0}\exp(2\gamma\theta)\,\|e(\theta)\|^2\,\mathrm{d}\theta \\ &\le \lambda_M(P)\,\|e(0)\|^2 + \lambda_M(\Gamma)\,\|e(0)\|^2\,\frac{\|\Omega\|^2}{\|e(0)\|^2}\int_{-\tau}^{0} \mathrm{e}^{2\gamma\theta}\mathrm{d}\theta \\ &= \left[\lambda_M(P) + \lambda_M(\Gamma)\frac{\|\Omega\|^2}{\|e(0)\|^2}\,\frac{1-\exp(-2\gamma\tau)}{2\gamma}\right]\|e(0)\|^2, \end{aligned}$$

where $\|\Omega\| = \sup_{-\tau\le\theta\le 0}\|e(\theta)\|$, and $V(e(t)) \ge \exp(2\gamma t)e^{\mathrm{T}}(t) \times Pe(t) \ge \exp(2\gamma t)\lambda_m(P)\,\|e(t)\|^2$; therefore, the convergence rates of the error states between the drive system (1) and the response system (4) are

$$\|e(t)\| = \sqrt{\frac{\lambda_M(P)}{\lambda_m(P)} + \frac{\lambda_M(\Gamma)}{\lambda_m(P)}\,\frac{\|\Omega\|^2}{\|e(0)\|^2}\,\frac{1-\exp(-2\gamma\tau)}{2\gamma}} \times \|e(0)\|^2\exp(-\gamma t). \tag{13}$$

From Definition 1, one concludes that the drive system (1) and the response system (4) are exponentially synchronized with an exponential synchronization rate γ. This thus completes the proof. □

Remark 3. Eq. (10) in Theorem 1 is nonlinear matrix inequality with respect to the parameters X, S, T, γ, Y_1, and Y_2. There are no efficient algorithms and computer software to solve this inequality. However, while γ is fixed, Eq. (10) is an LMI over the unknown parameters. Hence, Theorem 1 provides a design procedure for a synchronization controller for systems (1) and (4) with a given exponential synchronization rate. On the other hand, we will further derive some exponential synchronization conditions for systems (1) and (4), which are represented in the form of LMIs, which can be efficiently solved using existing algorithms.

Theorem 2. *If there exist positive definite matrices X, S, N_1, and N_2, diagonal semi-positive definite matrix T, a positive scalar $0 < \alpha < 1$, and matrices Y_1 and Y_2, which satisfy the following generalized eigenvalue problem (GEVP):*

$$\text{minimize } \alpha, \tag{14}$$

$$\text{subject to } M = \begin{bmatrix} M_{11} & M_{12} & M_{13} \\ * & M_{22} & M_{23} \\ * & * & M_{33} \end{bmatrix} < 0, \tag{15}$$

$$\frac{1}{\tau}X < \alpha\left(N_1 + \frac{1}{\tau}X\right), \tag{16}$$

$$N_2 < \alpha S, \tag{17}$$

where $0 < \alpha = \exp(-2\gamma\tau) < 1$, $\gamma > 0$, then the drive system (1) and the response system (4) can be globally exponentially synchronized. Moreover, the feedback gains are obtained as $K_1 = Y_1X^{-1}$ and $K_2 = Y_2X^{-1}$. The submatrices of M are $M_{11} = (AX - Y_1)^{\mathrm{T}} + AX - Y_1 + N_1 + S$, $M_{12} = A_dX - Y_2$, $M_{13} = B_pT + XC_q^{\mathrm{T}}(Q+H)$, $M_{22} = -N_2$, $M_{23} = XC_{qd}^{\mathrm{T}}(Q+H)$, $M_{33} = TD_p^{\mathrm{T}}(Q+H) + (Q+H)D_pT - 2T$, where $Q = \mathrm{diag}(q_1, q_2, \cdots, q_L)$, $H = \mathrm{diag}(h_1, h_2, \ldots, h_L)$.

Proof. By virtue of (16) and (17), we have

$$\begin{aligned} 0 &< 2\gamma X = (1+2\gamma\tau)\frac{1}{\tau}X - \frac{1}{\tau}X < \exp(2\gamma\tau)\frac{1}{\tau}X - \frac{1}{\tau}X \\ &= \frac{1}{\alpha}\cdot\frac{1}{\tau}X - \frac{1}{\tau}X < N_1, \end{aligned} \tag{18}$$

$$0 < N_2 < \alpha S = \exp(-2\gamma\tau)S. \tag{19}$$

From (18) and (19), we obtain the equation given in Box V.

Hence, if (15) holds, (10) is also satisfied. According to Theorem 1, we can judge that the drive system (1) and the response system (4) are globally exponentially synchronized. It is well known that if the exponential synchronization rate γ is maximal (or α is minimal), the error dynamical system (9) converges to the trivial solution as quickly as possible. This requires solving the generalized eigenvalue minimization problem (14)–(17), which is a quasi-convex optimization problem and can be solved by using the MATLAB LMI Control Toolbox (Gahinet et al., 1995). The proof of Theorem 2 is thus completed. □

Remark 4. In fact, Theorem 2 provides a design approach to achieve an optimal synchronization controller and the optimal exponential synchronization rate. The optimal controller ensures that the drive system (1) and the response system (4) can be globally exponentially synchronized at fast speed.

$$R_i = \begin{bmatrix} 0 & 0 & 0 & \cdots & 0 & -C_{q,i}^{\mathrm{T}} s_i & 0 & \cdots & 0 \\ 0 & 0 & 0 & \cdots & 0 & -C_{qd,i}^{\mathrm{T}} s_i & 0 & \cdots & 0 \\ 0 & 0 & 0 & \cdots & 0 & -d_{p,i,1} s_i & 0 & \cdots & 0 \\ \vdots & \vdots & \vdots & \vdots & \vdots & \vdots & \vdots & \vdots & \vdots \\ 0 & 0 & 0 & \cdots & 0 & -d_{p,i,i-1} s_i & 0 & \cdots & 0 \\ -s_i C_{q,i} & -s_i C_{qd,i} & -s_i d_{p,i,1} & \cdots & -s_i d_{p,i,i-1} & 2 - 2 s_i d_{p,i,i} & s_i d_{p,i,i+1} & \cdots & s_i d_{p,i,L} \\ 0 & 0 & 0 & \cdots & 0 & d_{p,i,i+1} s_i & 0 & \cdots & 0 \\ \vdots & \vdots & \vdots & \vdots & \vdots & \vdots & \vdots & \vdots & \vdots \\ 0 & 0 & 0 & \cdots & 0 & d_{p,i,L} s_i & 0 & \cdots & 0 \end{bmatrix}, \quad i = 1, \ldots, L$$

Box III.

$$\begin{aligned} R_0 - \sum_{i=1}^{L} \varepsilon_i R_i &= \begin{bmatrix} (A-K_1)^{\mathrm{T}} P + P(A-K_1) + 2\gamma P + \Gamma & P(A_d - K_2) & PB_p \\ (A_d - K_2)^{\mathrm{T}} P & -\exp(-2\gamma\tau)\Gamma & 0 \\ B_p^{\mathrm{T}} P & 0 & 0 \end{bmatrix} \\ &\quad - \begin{bmatrix} 0 & 0 & -C_q^{\mathrm{T}}(Q+H)\Sigma \\ 0 & 0 & -C_{qd}^{\mathrm{T}}(Q+H)\Sigma \\ -\Sigma(Q+H)C_q & -\Sigma(Q+H)C_q & 2\Sigma - D_p^{\mathrm{T}}(Q+H)\Sigma - \Sigma(Q+H)D_p \end{bmatrix} \\ &= \begin{bmatrix} (A-K_1)^{\mathrm{T}} P + P(A-K_1) + 2\gamma P + \Gamma & P(A_d - K_2) & PB_p + C_q^{\mathrm{T}}(Q+H)\Sigma \\ (A_d - K_2)^{\mathrm{T}} P & -\exp(-2\gamma\tau)\Gamma & C_{qd}^{\mathrm{T}}(Q+H)\Sigma \\ B_p^{\mathrm{T}} P + \Sigma(Q+H)C_q & \Sigma(Q+H)C_q & D_p^{\mathrm{T}}(Q+H)\Sigma + \Sigma(Q+H)D_p - 2\Sigma \end{bmatrix} < 0 \end{aligned}$$

Box IV.

$$\begin{aligned} &\begin{bmatrix} (AX - Y_1)^{\mathrm{T}} + AX - Y_1 + 2\gamma X + S & A_d X - Y_2 & B_p T + X C_q^{\mathrm{T}}(Q+H) \\ * & -\exp(-2\gamma\tau) S & X C_{qd}^{\mathrm{T}}(Q+H) \\ * & * & T D_p^{\mathrm{T}}(Q+H) + (Q+H) D_p T - 2T \end{bmatrix} \\ &\quad - \begin{bmatrix} (AX - Y_1)^{\mathrm{T}} + AX - Y_1 + N_1 + S & A_d X - Y_2 & B_p T + X C_q^{\mathrm{T}}(Q+H) \\ * & -N_2 & X C_{qd}^{\mathrm{T}}(Q+H) \\ * & * & T D_p^{\mathrm{T}}(Q+H) + (Q+H) D_p T - 2T \end{bmatrix} \\ &= \begin{bmatrix} 2\gamma X - N_1 & 0 & 0 \\ 0 & N_2 - \exp(-2\gamma\tau) S & 0 \\ 0 & 0 & 0 \end{bmatrix} \le 0 \end{aligned}$$

Box V.

Remark 5. For convenience of the application of designed controllers in engineering practice, it is necessary to limit the magnitude of feedback gains K_1 and K_2, which is equivalent to restricting the norms of X, Y_1, and Y_2 in some ranges; that is,

$$\begin{cases} \|X^{-1}\| < \delta, \\ \|Y_1\| < \lambda_1, \\ \|Y_2\| < \lambda_2, \end{cases} \tag{20}$$

where δ, λ_1 and λ_2 are positive scalars, which are well chosen according to the design requirement in practical chaotic systems. By virtue of the well-known Schur complement formula (Boyd et al., 1994), the constraints (20) are equivalent to

$$\begin{bmatrix} -\delta X & I \\ I & -\delta X \end{bmatrix} < 0, \tag{21}$$

$$\begin{bmatrix} -\lambda_1 I & Y_1^{\mathrm{T}} \\ Y_1 & -\lambda_1 I \end{bmatrix} < 0, \tag{22}$$

$$\begin{bmatrix} -\lambda_2 I & Y_2^{\mathrm{T}} \\ Y_2 & -\lambda_2 I \end{bmatrix} < 0. \tag{23}$$

If $A_d = 0$ and $C_{qd} = 0$, system (1) is a chaotic neural network without delays, which is represented as

$$\begin{cases} \dot{x}(t) = Ax(t) + B_p \phi(\xi(t)), \\ \xi(t) = C_q x(t) + D_p \phi(\xi(t)), \end{cases} \tag{24}$$

The response system corresponding to the drive system (24) is given by the following equations:

$$\begin{cases} \dot{y}(t) = Ay(t) + B_p \phi(\zeta(t)) + u(t), \\ \zeta(t) = C_q y(t) + D_p \phi(\zeta(t)), \end{cases} \tag{25}$$

The exponential synchronization controller is of the form

$$u(t) = Ke(t), \tag{26}$$

where $K \in \Re^{n \times n}$ is the state feedback gain. With the control law (26), the error dynamical system between (24) and (25) can be expressed in the following form:

$$\begin{cases} \dot{e}(t) = (A - K)e(t) + B_p \psi(\eta(t)), \\ \eta(t) = C_q e(t) + D_p \psi(\eta(t)), \end{cases} \tag{27}$$

Since $\psi(0) = 0$, system (27) has a trivial solution: $e(t) \equiv 0$. For the drive system (24) and the response system (25), we can use the following corollaries to design an exponential synchronization controller.

Corollary 1. *If there exist positive definite matrix X, diagonal semi-positive definite matrix T, a positive scalar γ, and a matrix Y, which satisfy the following nonlinear matrix inequality,*

$$\begin{bmatrix} (AX-Y)^{\mathrm{T}}+AX-Y+2\gamma X & B_pT+XC_q^{\mathrm{T}}(Q+H) \\ * & TD_p^{\mathrm{T}}(Q+H)+(Q+H)D_pT-2T \end{bmatrix} < 0, \tag{28}$$

where $Q = \mathrm{diag}(q_1, q_2, \ldots, q_L)$, $H = \mathrm{diag}(h_1, h_2, \ldots, h_L)$, then the drive system (24) and the response system (25) can be synchronized with an exponential synchronization rate of γ. Moreover, the feedback gain is obtained as $K = YX^{-1}$.

Corollary 2. *If there exist positive definite matrices X and N, diagonal semi-positive definite matrix T, a positive scalar α, and a matrix Y, which satisfy the following GEVP,*

$$\text{minimize } \alpha, \tag{29}$$

subject to

$$\begin{bmatrix} (AX-Y)^{\mathrm{T}}+AX-Y+N & B_pT+XC_q^{\mathrm{T}}(Q+H) \\ * & TD_p^{\mathrm{T}}(Q+H)+(Q+H)D_pT-2T \end{bmatrix} < 0, \tag{30}$$

$$2X < \alpha N, \tag{31}$$

where $\alpha = 1/\gamma$, $\gamma > 0$, $Q = \mathrm{diag}(q_1, q_2, \ldots, q_L)$, $H = \mathrm{diag}(h_1, h_2, \ldots, h_L)$, then the drive system (24) and the response system (25) can be globally exponentially synchronized. Furthermore, the feedback gain is obtained as $K = YX^{-1}$.

The proofs of Corollaries 1 and 2 follow the same ideas as those in the proofs of Theorems 1 and 2, and thus are omitted here. For Corollary 1, the following Lyapunov functional is chosen: $V(x) = \mathrm{e}^{2\gamma t}x(t)^{\mathrm{T}}Px(t)$.

4. Illustrative examples

In this section, we investigate the problem of global exponential synchronization for three chaotic neural networks (a chaotic CNN without delays, a chaotic delayed Hopfield neural network, and a chaotic delayed RMLP), and compare our results to those in other references in some detail, to demonstrate that the approaches developed here are not only very convenient to implement in practice, but also further extend the ideas and techniques presented in recent literature.

Example 1. Consider a chaotic CNN without delays as follows (Zou & Nossek, 1993):

$$\begin{bmatrix}\dot{x}_1(t)\\ \dot{x}_2(t)\\ \dot{x}_3(t)\end{bmatrix} = -\begin{bmatrix}x_1(t)\\ x_2(t)\\ x_3(t)\end{bmatrix} + \begin{bmatrix}1.25 & -3.2 & -3.2\\ -3.2 & 1.1 & -4.4\\ -3.2 & 4.4 & 1\end{bmatrix}\begin{bmatrix}f(x_1(t))\\ f(x_2(t))\\ f(x_3(t))\end{bmatrix}, \tag{32}$$

where $f(x_i(t)) = (|x_i(t)+1| - |x_i(t)-1|)/2$, $i = 1, 2, 3$. As shown in Fig. 1, the CNN (32) exhibits a chaotic behavior (Cheng et al., 2005; Lu & Leeuwen, 2006; Zou & Nossek, 1993). Now the response chaotic CNN is designed as follows:

$$\begin{bmatrix}\dot{y}_1(t)\\ \dot{y}_2(t)\\ \dot{y}_3(t)\end{bmatrix} = -\begin{bmatrix}y_1(t)\\ y_2(t)\\ y_3(t)\end{bmatrix} + \begin{bmatrix}1.25 & -3.2 & -3.2\\ -3.2 & 1.1 & -4.4\\ -3.2 & 4.4 & 1\end{bmatrix}\begin{bmatrix}f(y_1(t))\\ f(y_2(t))\\ f(y_3(t))\end{bmatrix} + u(t). \tag{33}$$

We convert the CNN (33) into system (25), where $y = [\,y_1(t)\quad y_2(t)\quad y_3(t)\,]^{\mathrm{T}}$, $A = \mathrm{diag}(-1, -1, -1)$,

$$B_p = \begin{bmatrix}1.25 & -3.2 & -3.2\\ -3.2 & 1.1 & -4.4\\ -3.2 & 4.3 & 1\end{bmatrix},$$

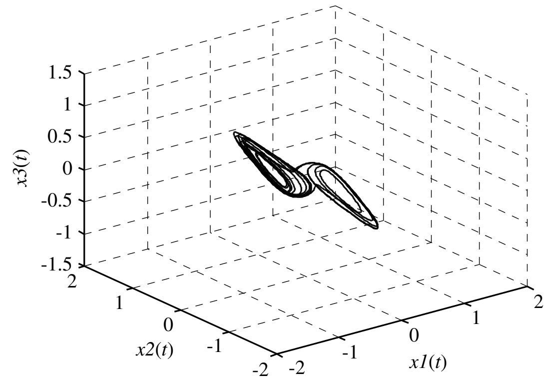

Fig. 1. The chaotic behavior of CNN (32) with the initial condition $[x_1(0)\,x_2(0)\,x_3(0)]^{\mathrm{T}} = [0.1\;0.1\;0.1]^{\mathrm{T}}$ in Example 1.

$C_q = I_{3\times3}$, $D_p = 0_{3\times3}$, $Q = 0_{3\times3}$, $H = I_{3\times3}$, $\phi_i(\zeta_i(t)) = f(y_i(t))$, $i = 1, 2, 3$. The controller (26) is adopted to synchronize the CNNs (32) and (33), where $u(t) \in \mathfrak{R}^3$ and $K \in \mathfrak{R}^{3\times3}$. According to Corollary 2, solving the GEVP (29)–(31), we obtain the solutions of the GEVP and the feedback gain as

$$\alpha = 6.8265\times10^{-7},\qquad \gamma = 1.4649\times10^{6},$$

$$X = 10^{-9}\times\begin{bmatrix}0.1488 & -0.0099 & -0.0568\\ -0.0099 & 0.1500 & -0.0045\\ -0.0568 & -0.0045 & 0.0332\end{bmatrix},$$

$$N = 10^{3}\times\begin{bmatrix}0.8702 & -0.0557 & -0.3320\\ -0.0557 & 0.8807 & -0.0274\\ -0.3320 & -0.0274 & 0.1946\end{bmatrix},$$

$$Y = \begin{bmatrix}0.9667 & -0.6083 & -1.7742\\ 0.9007 & 1.2603 & -14.0871\\ 0.8032 & 14.7741 & 1.2283\end{bmatrix},$$

$$T = \mathrm{diag}(0.1334, 0.0759, 0.1017),$$

$$K = 10^{12}\times\begin{bmatrix}-0.0435 & -0.0108 & -0.1292\\ -0.4674 & -0.0594 & -1.2306\\ 0.0937 & 0.1110 & 0.2121\end{bmatrix}.$$

Therefore, we can conclude that the chaotic CNNs (32) and (33) are synchronized with an exponential convergence rate of 1.4649×10^{6}. Since the feedback gain $\|K\| = 1.3458e\times10^{12}$ is too large to implement in practice, we must restrict the norm of feedback gain in a certain range, therefore we solve the GEVP (29)–(31) with the following constraints:

$$\begin{bmatrix}-\delta X & I\\ I & -\delta X\end{bmatrix} < 0, \tag{34}$$

$$\begin{bmatrix}-\lambda I & Y^{\mathrm{T}}\\ Y & -\lambda I\end{bmatrix} < 0, \tag{35}$$

where $\delta = 5$ and $\lambda = 5$. We get the following solutions of (29)–(31), (34) and (35), and the feedback gain K as

$$\alpha = 0.0494,\qquad \gamma = 20.2580,$$

$$X = \begin{bmatrix}0.2065 & 0.0011 & 0.0084\\ 0.0011 & 0.2010 & 0.0005\\ 0.0084 & 0.0005 & 0.2122\end{bmatrix},$$

$$N = 10^{3}\times\begin{bmatrix}0.8702 & -0.0557 & -0.3320\\ -0.0557 & 0.8807 & -0.0274\\ -0.3320 & -0.0274 & 0.1946\end{bmatrix},$$

$$Y = \begin{bmatrix}8.5608 & 0.0749 & 0.5727\\ 0.0749 & 8.1834 & 0.0175\\ 0.5727 & 0.0175 & 8.9236\end{bmatrix},$$

$$T = \mathrm{diag}(0.0326, 0.0233, 0.0901),$$

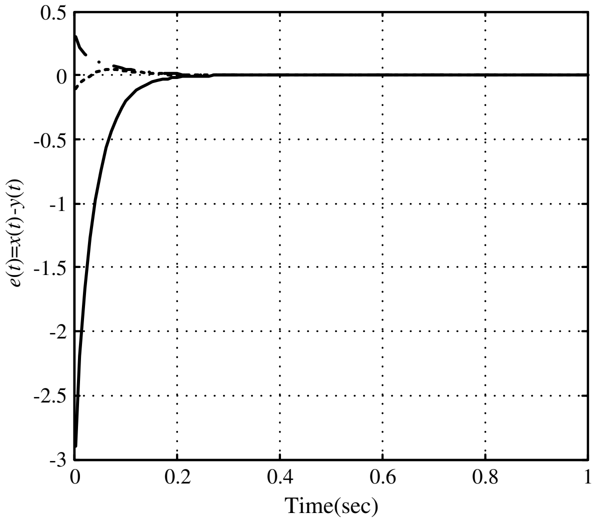

Fig. 2. The waveform of synchronization errors $e_1(t) = x_1(t) - y_1(t)$ (solid line), $e_2(t) = x_2(t) - y_2(t)$ (dashed line), and $e_3(t) = x_3(t) - y_3(t)$ (dot–dashed line) in Example 1.

$$K = \begin{bmatrix} 23.8248 & -0.2011 & -1.4629 \\ -0.2027 & 24.7789 & -0.0420 \\ -1.4653 & -0.0400 & 22.8883 \end{bmatrix}.$$

Fig. 2 depicts the synchronization errors of the state variables between the drive system (32) and the response (33) under a state feedback controller with the second gain K for the initial condition $[0.1\ 0.1\ 0.1]^{\mathrm{T}}$ and $[3\ 0.2\ \ -0.2]^{\mathrm{T}}$, respectively. Comparing Fig. 2 with Fig. 2 in Cheng et al. (2005) and Fig. 5 in Lu and Leeuwen (2006), here we could obtain a larger convergence rate than Cheng et al. (2005) and Lu and Leeuwen (2006), where the dynamical errors converge to zeros within 0.3 s. Therefore, we can achieve an optimal controller, while Cheng et al. (2005) and Lu and Leeuwen (2006) cannot. On the other hand, the feedback gains in Cheng et al. (2005) and Lu and Leeuwen (2006) are obtained by trial, while our controller parameters can be solved by the MATLAB LMI Control Toolbox (Gahinet et al., 1995).

Example 2. Consider the following delayed Hopfield neural networks with two neurons (Lu, 2002):

$$\begin{bmatrix} \dot{x}_1(t) \\ \dot{x}_2(t) \end{bmatrix} = -\begin{bmatrix} x_1(t) \\ x_2(t) \end{bmatrix} + \begin{bmatrix} 2 & -0.1 \\ -5 & 4.5 \end{bmatrix} \begin{bmatrix} f(x_1(t)) \\ f(x_2(t)) \end{bmatrix} + \begin{bmatrix} -1.5 & -0.1 \\ -0.2 & -4 \end{bmatrix} \begin{bmatrix} f(x_1(t-1)) \\ f(x_2(t-1)) \end{bmatrix}, \tag{36}$$

where $f(x) = \tanh(x)$. Fig. 3 shows the chaotic behavior of system (36) with the initial condition $[x_1(s)\ x_2(s)]^{\mathrm{T}} = [0.4\ 0.6]^{\mathrm{T}}$ for $-1 \le s \le 0$. The response chaotic delayed Hopfield neural network is designed as follows:

$$\begin{bmatrix} \dot{y}_1(t) \\ \dot{y}_2(t) \end{bmatrix} = -\begin{bmatrix} y_1(t) \\ y_2(t) \end{bmatrix} + \begin{bmatrix} 2 & -0.1 \\ -5 & 4.5 \end{bmatrix} \begin{bmatrix} f(y_1(t)) \\ f(y_2(t)) \end{bmatrix} + \begin{bmatrix} -1.5 & -0.1 \\ -0.2 & -4 \end{bmatrix} \begin{bmatrix} f(y_1(t-1)) \\ f(y_2(t-1)) \end{bmatrix} + u(t). \tag{37}$$

We convert the delayed Hopfield neural network (37) into system (4), where $y = [y_1(t)\quad y_2(t)]^{\mathrm{T}}$, $A = \mathrm{diag}(-1, -1)$, $A_d = 0_{3\times 3}$, $B_p = \begin{bmatrix} 2 & -0.1 & -1.5 & -0.1 \\ -5 & 4.5 & -0.2 & -4 \end{bmatrix}$, $C_q = \begin{bmatrix} 1 & 0 \\ 0 & 1 \\ 0 & 0 \\ 0 & 0 \end{bmatrix}$, $C_{qd} = \begin{bmatrix} 0 & 0 \\ 0 & 0 \\ 1 & 0 \\ 0 & 1 \end{bmatrix}$, $D_p = 0_{4\times 4}$, $Q = 0_{4\times 4}$, $H = I_{4\times 4}$, $\phi_1(\zeta_1(t)) = \tanh(y_1(t))$, $\phi_2(\zeta_2(t)) = \tanh(y_2(t))$, $\phi_3(\zeta_3(t)) = \tanh(y_1(t-1))$, $\phi_4(\zeta_4(t)) = \tanh(y_2(t-1))$. The controller (8) is employed to synchronize the delayed Hopfield neural networks (36) and (37), where $u(t) \in \Re^2$, $K_1 \in \Re^{2\times 2}$, and $K_2 \in \Re^{2\times 2}$. According to Theorem 2, solving the GEVP (14)–(17) with the constraints (21)–(23), where $\delta = 5$, $\lambda_1 = 8$ and $\lambda_2 = 8$, we obtain the solutions of the GEVP and the feedback gain as

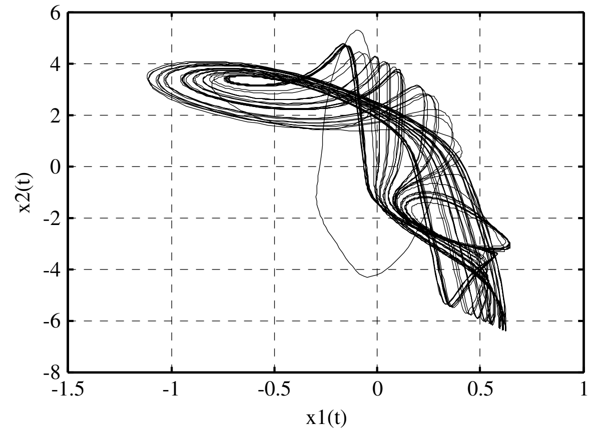

Fig. 3. The chaotic behavior of the delayed Hopfield neural network (36) with the initial condition $[x_1(s)\ x_2(s)]^{\mathrm{T}} = [0.4\ 0.6]^{\mathrm{T}}$ for $-1 \le s \le 0$, in Example 2.

$$\alpha = 0.0219, \qquad \gamma = 45.6402, \qquad X = \begin{bmatrix} 0.2059 & 0.0007 \\ 0.0007 & 0.2003 \end{bmatrix},$$

$$N_1 = \begin{bmatrix} 9.5647 & 0.0717 \\ 0.0717 & 8.9636 \end{bmatrix},$$

$$N_2 = \begin{bmatrix} 0.0299 & 0.0017 \\ 0.0017 & 0.0583 \end{bmatrix}, \qquad S = \begin{bmatrix} 1.7936 & 0.1213 \\ 0.1213 & 2.6851 \end{bmatrix},$$

$$Y_1 = \begin{bmatrix} 7.7886 & -0.0219 \\ -0.0219 & 7.9887 \end{bmatrix},$$

$$Y_2 = \begin{bmatrix} -0.1545 & -0.0106 \\ -0.0221 & -0.4007 \end{bmatrix},$$

$$T = \mathrm{diag}(0.0085, 0.0460, 1.3140, 0.3470),$$

$$K_1 = \begin{bmatrix} 37.8273 & -0.2508 \\ -0.2514 & 39.8807 \end{bmatrix}, \qquad K_2 = \begin{bmatrix} -0.7499 & -0.0500 \\ -0.1000 & -2.0000 \end{bmatrix}.$$

Fig. 4 depicts the synchronization errors of the state variables between the drive system (36) and the response (37) with the initial condition $[x_1(s)\ x_2(s)]^{\mathrm{T}} = [0.4\ 0.6]^{\mathrm{T}}$ and $[0.45\ 0.55]^{\mathrm{T}}$, for $-1 \le s \le 0$, respectively. Comparing Fig. 4 with Fig. 6 in Cheng et al. (2005) and Figs. 2–4 in Lu and Leeuwen (2006), we can see that systems (36) and (37) have been synchronized with a higher exponential synchronization rate than in Cheng et al. (2005) and Lu and Leeuwen (2006). In addition, we can get the optimal controller according to our requirement of performance, or implementation in practice. It is flexible and easy to change some parameters in Theorems 1 and 2, such as δ, λ_1 and λ_2, to satisfy such requirements.

Example 3. We consider the following chaotic delayed RMLP:

$$\dot{x}(t) = \tanh(W_A \tanh(V_A x(t)) + W_B \tanh(V_B x(t-1))), \tag{38}$$

with the initial value $x_1(0) = 0.2$, $x_2(0) = 0.2$ and $x_3(0) = 0.2$, where

$$W_A = \begin{bmatrix} 3 & 0.02 & 0 \\ 0 & 3 & 0 \\ 0 & 0 & 1 \end{bmatrix}, \qquad V_A = \begin{bmatrix} 1 & 0 & 0 \\ 0 & 1.5 & 0 \\ 0 & 0 & 2 \end{bmatrix},$$

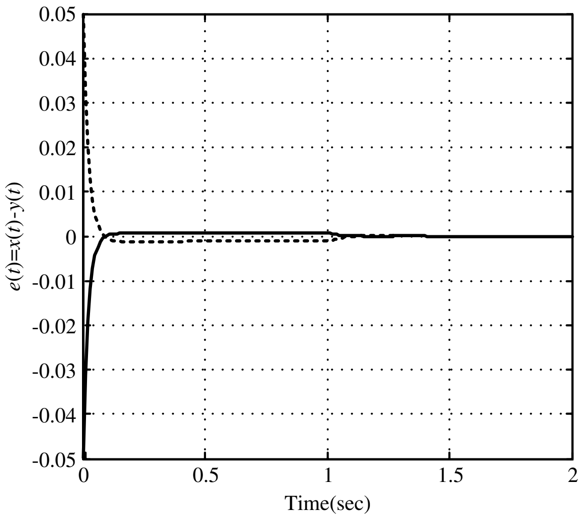

Fig. 4. The waveform of synchronization errors $e_1(t) = x_1(t) - y_1(t)$ (solid line), and $e_2(t) = x_2(t) - y_2(t)$ (dashed line) in Example 2.

$$W_B = \begin{bmatrix} -5.8 & 0 & 0.785 \\ 0 & -5.8 & 0.785 \\ 0 & 0 & -5.8 \end{bmatrix}, \qquad V_B = \begin{bmatrix} 1 & 0 & 1 \\ 0 & 1.5 & 0 \\ 1 & 1.2 & 2 \end{bmatrix}.$$

The behavior of the chaotic RMLP (38) is shown in Fig. 5. The response chaotic delayed RMLP is designed as follows:

$$\dot{y}(t) = \tanh(W_A \tanh(V_A y(t)) + W_B \tanh(V_B y(t-1))) + u(t). \quad (39)$$

We transform the delayed RMLP (39) into system (4), where

$$A = 0_{3\times3}, \qquad A_d = 0_{3\times3}, \qquad B_p = \begin{bmatrix} I_{3\times3} & 0_{3\times3} & 0_{3\times3} \end{bmatrix},$$

$$C_q = \begin{bmatrix} 0_{3\times3} \\ V_A \\ 0_{3\times3} \end{bmatrix},$$

$$C_{qd} = \begin{bmatrix} 0_{3\times3} \\ 0_{3\times3} \\ V_B \end{bmatrix}, \qquad D_p = \begin{bmatrix} 0_{3\times3} & W_A & W_B \\ 0_{3\times3} & 0_{3\times3} & 0_{3\times3} \\ 0_{3\times3} & 0_{3\times3} & 0_{3\times3} \end{bmatrix},$$

$$Q = 0_{9\times9}, \qquad H = I_{9\times9},$$

$$\begin{bmatrix} \phi_1(\zeta_1(t)) & \phi_2(\zeta_2(t)) & \phi_3(\zeta_3(t)) \end{bmatrix}^{\mathrm{T}} = \tanh(W_A \tanh(V_A) y(t)) + W_B \tanh(V_B y(t-1)),$$

$$\begin{bmatrix} \phi_4(\zeta_4(t)) & \phi_5(\zeta_5(t)) & \phi_6(\zeta_6(t)) \end{bmatrix}^{\mathrm{T}} = \tanh(V_A y(t)),$$

$$\begin{bmatrix} \phi_7(\zeta_7(t)) & \phi_8(\zeta_8(t)) & \phi_9(\zeta_9(t)) \end{bmatrix}^{\mathrm{T}} = \tanh(V_B y(t-1)).$$

The controller (8) is employed to synchronize the delayed RMLPs (38) and (39), where $u(t) \in \mathfrak{R}^3$, $K_1 \in \mathfrak{R}^{3\times3}$, and $K_2 \in \mathfrak{R}^{3\times3}$. According to Theorem 2, solving the GEVP (14)–(17) with the constraints (21)–(23), where $\delta = 5$, $\lambda_1 = 6$ and $\lambda_2 = 6$, we obtain the solutions of the GEVP and the feedback gain as

$$\alpha = 0.1523, \qquad \gamma = 6.5642,$$

$$X = \begin{bmatrix} 0.2523 & -0.0002 & -0.0283 \\ -0.0002 & 0.2134 & -0.0059 \\ -0.0283 & -0.0059 & 0.2185 \end{bmatrix},$$

$$N_1 = \begin{bmatrix} 1.8483 & -0.1467 & -0.3177 \\ -0.1467 & 1.6430 & -0.1138 \\ -0.3177 & -0.1138 & 1.3393 \end{bmatrix},$$

$$N_2 = \begin{bmatrix} 0.3390 & 0.0502 & 0.2306 \\ 0.0502 & 0.6496 & 0.1528 \\ 0.2306 & 0.1528 & 0.4953 \end{bmatrix},$$

$$S = \begin{bmatrix} 2.6798 & 0.2142 & 1.3372 \\ 0.2142 & 4.6432 & 0.9335 \\ 1.3372 & 0.9335 & 3.3791 \end{bmatrix},$$

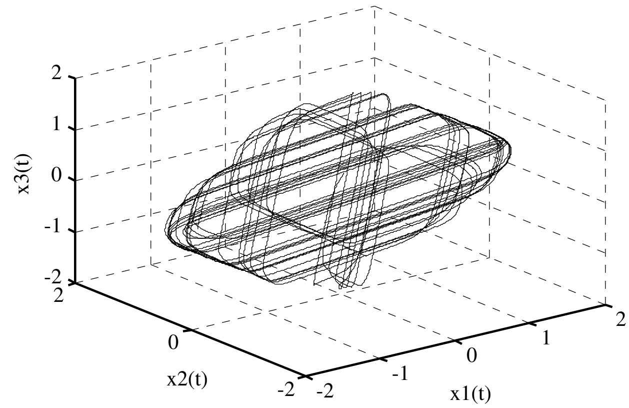

Fig. 5. The chaotic behavior of the delayed RMLP (38) with the initial condition $[x_1(s)\ x_2(s)\ x_3(s)]^{\mathrm{T}} = [0.2\ 0.2\ 0.2]^{\mathrm{T}}$, for $-1 \le s \le 0$, in Example 3.

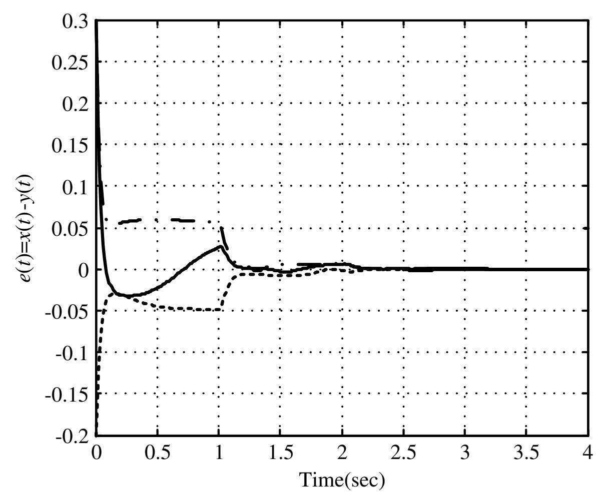

Fig. 6. The waveform of synchronization errors $e_1(t) = x_1(t) - y_1(t)$ (solid line), $e_2(t) = x_2(t) - y_2(t)$ (dashed line), and $e_3(t) = x_3(t) - y_3(t)$ (dot–dashed line) in Example 3.

$$Y_1 = \begin{bmatrix} 5.8079 & 0.0551 & 0.0708 \\ 0.0551 & 5.8067 & 0.0364 \\ 0.0708 & 0.0364 & 5.9429 \end{bmatrix},$$

$$Y_2 = \begin{bmatrix} -0.4982 & 0.1388 & -0.2804 \\ 0.1128 & -0.7804 & 0.2687 \\ -0.4281 & -0.4818 & -0.9555 \end{bmatrix},$$

$$T = \mathrm{diag}(6.2922, 4.0856, 8.0481, 0.1060, 0.1641, 0.5362, 0.2965, 0.1646, 0.3361),$$

$$K_1 = \begin{bmatrix} 23.3979 & 0.3767 & 3.3649 \\ 0.3497 & 27.2359 & 0.9519 \\ 3.3845 & 0.9437 & 27.6627 \end{bmatrix},$$

$$K_2 = \begin{bmatrix} -2.1475 & 0.6050 & -1.5450 \\ 0.5791 & -3.6226 & 1.2062 \\ -2.2291 & -2.3914 & -4.7265 \end{bmatrix}.$$

When the state feedback law (8) with the above K_1 and K_2 is put on the unforced error dynamical system between the drive system (38) and the response system (39) with the initial condition $[x_1(s)\ x_2(s)\ x_3(s)]^{\mathrm{T}} = [0.2\ 0.2\ 0.2]^{\mathrm{T}}$ and $[y_1(s)\ y_2(s)\ y_3(s)]^{\mathrm{T}} = [-0.1\ 0.4\ -0.1]^{\mathrm{T}}$, for $-1 \le s \le 0$, respectively, the synchronization errors of the state variables converge to zero exponentially, which is shown in Fig. 6.

From Example 3, we have noticed that, although Cheng et al. (2005), Lu and Leeuwen (2006), Lu and Cao (2007), Sun and Cao (2007), Sun et al. (2007) and Zhou et al. (2006) have provided a common chaotic neural network model to describe several well-known dynamic neural networks, and give some explicit design procedures for synchronization controller of this chaotic neural network model, this model could not include RMLPs, and their approaches could not be used in the synchronization synthesis of chaotic RMLPs.

5. Conclusion

In this paper, we provide a general chaotic neural network model to unify several well-known dynamic neural networks with or without delays. Utilizing time-delay feedback control and LMI techniques, we have proposed several criteria to design optimal exponential synchronization controllers of this general chaotic neural network model. Solving the GEVPs by using the MATLAB LMI Control Toolbox (Gahinet et al., 1995), we have obtained the optimal exponential synchronization rates and the feedback gain matrices of optimal controllers in the response networks, with which the drive systems and the response systems can be exponentially synchronized as quickly as possible. Finally, some illustrative examples with their simulations have been utilized to demonstrate the effectiveness of the proposed methods. In addition, the design approaches can be easily extended to synthesize synchronization controllers for any chaotic system as long as the equations can be transformed into the general model, (1). We believe that our results should provide some practical guidelines for engineering applications of chaos.

References

Aihara, K., Takabe, T., & Toyoda, M. (1990). Chaotic neural networks. *Physics Letters A*, *144*(6–7), 333–340.

Barabanov, N. E., & Prokhorov, D. V. (2002). Stability analysis of discrete-time recurrent neural networks. *IEEE Transactions on Neural Networks*, *13*(2), 292–303.

Boyd, S. P., Ghaoui, L. E., Feron, E., & Balakrishnan, V. (1994). *Linear matrix inequalities in system and control theory*. Philadelphia, PA: Society for Industrial Applied Mathematics (SIAM).

Bueno, L. P. P., & Araujo, A. F. R. (2006). Controlling chaos in chaotic bidirectional associative memories. In *International joint conference on neural networks* (pp. 3983–3990).

Cao, J., Li, H. X., & Ho, Daniel W. C. (2005). Synchronization criteria of Lur'e systems with time-delay feedback control. *Chaos, Solitons and Fractals*, *23*(4), 1285–1298.

Chen, G., & Dong, X. (1998). *From chaos to order: Methodologies, perspectives, and applications*. Singapore: World Scientific Pub. Co..

Cheng, C.-J., Liao, T.-L., & Hwang, C.-C. (2005). Exponential synchronization of a class of chaotic neural network. *Chaos, Solitons and Fractals*, *24*(1), 197–206.

Chen, W.-H., Lu, X., & Chen, F. (2008). Impulsive synchronization of chaotic Lur'e systems via partial states. *Physics Letters A*, *372*(23), 4210–4216.

Cohen, M. A., & Grossberg, S. (1983). Absolute stability of global pattern formation and parallel memory storage by competitive neural network. *IEEE Transactions on Systems, Man, and Cybernetics*, *13*(5), 815–826.

Fradkov, A. L., & Evans, R. J. (2005). Control of chaos: Methods and applications in engineering. *Annual Reviews in Control*, *29*(1), 33–56.

Gahinet, P., Nemirovsky, A., Laub, A. J., & Chilali, M. (1995). *LMI control toolbox — for use with Matlab*. Natick, MA: The MATH Works, Inc..

Gilli, M. (1993). Strange attractors in delayed cellular neural networks. *IEEE Transactions on Circuits and Systems I: Fundamental Theory and Application*, *40*(11), 849–853.

Han, S. K., Kurrer, C., & Kuramoto, Y. (1995). Dephasing and bursting in coupled neural oscillators. *Physical Review Letters*, *75*(17), 3190–3193.

He, G., Cao, Z., Zhu, P., & Ogura, H. (2003). Controlling chaos in a chaotic neural network. *Neural Networks*, *16*(8), 1195–1200.

He, W., & Cao, J. (2008). Adaptive synchronization of a class of chaotic neural networks with known or unknown parameters. *Physics Letters A*, *372*(4), 408–416.

Kwok, T., & Smith, K. A. (2000). Experimental analysis of chaotic neural network models for combinatorial optimization under a unifying framework. *Neural Networks*, *13*(7), 731–744.

Liao, X., & Chen, G. (2003). Chaos synchronization of general Lur'e systems via time-delay feedback control. *International Journal of Bifurcation and chaos*, *13*(1), 207–213.

Liao, X. F., Chen, G. R., & Sanchez, E. N. (2002a). Delay-dependent exponential stability analysis of delayed neural networks: An LMI approach. *Neural Networks*, *15*(7), 855–866.

Liao, X. F., Chen, G. R., & Sanchez, E. N. (2002b). LMI-based approach for asymptotically stability analysis of delayed neural networks. *IEEE Transactions on Circuits and Systems I: Fundamental Theory and Application*, *49*(7), 1033–1039.

Li, T., Fei, S.-M., Zhu, Q., & Cong, S. (2008). Exponential synchronization of chaotic neural networks with mixed delays. *Neurocomputing*, *71*(13–15), 3005–3019.

Liu, M. Q. (2006). Discrete-time delayed standard neural network model and its application. *Science in China: Series F Information Sciences*, *49*(2), 137–154.

Liu, M. Q. (2007). Delayed standard neural network models for control systems. *IEEE Transactions on Neural Networks*, *18*(5), 1376–1391.

Lu, H., & Leeuwen, C. V. (2006). Synchronization of chaotic neural networks via output or state coupling. *Chaos, Solitons and Fractals*, *30*(1), 166–176.

Lu, H. T. (2002). Chaotic attractors in delayed neural networks. *Physics Letters A*, *298*(2–3), 109–116.

Lu, J., & Cao, J. (2007). Synchronization-based approach for parameters identification in delayed chaotic neural network. *Physica A: Statistical Mechanics and its Applications*, *382*(2), 672–682.

Milanovic, V., & Zaghloul, M. E. (1996). Synchronization of chaotic neural networks and applications to communications. *International Journal of Bifurcation and Chaos*, *6*(12B), 2571–2585.

Nesterov, Y., & Nemirovsky, A. (1994). *Interior point polynomial methods in convex programming: Theory and applications*. Philadelphia, PA: Society for Industrial Applied Mathematics (SIAM).

Pecora, L. M., & Carroll, T. L. (1990). Synchronization in chaotic systems. *Physical Review Letters*, *64*(8), 821–824.

Sun, Y., & Cao, J. (2007). Adaptive lag synchronization of unknown chaotic delayed neural networks with noise perturbation. *Physics Letters A*, *364*(3–4), 277–285.

Sun, Y., Cao, J., & Wang, Z. (2007). Exponential synchronization of stochastic perturbed chaotic delayed neural networks. *Neurocomputing*, *70*(13–15), 2477–2485.

Tang, Y., Qiu, R., Fang, J.-A, Miao, Q., & Xia, M. (2008). Adaptive lag synchronization in unknown stochastic chaotic neural networks with discrete and distributed time-varying delays. *Physics Letters A*, *372*(24), 4425–4433.

Tan, Z., & Ali, M. K. (2001). Associative memory using synchronization in a chaotic neural network. *International Journal of Modern Physics C*, *12*(1), 19–29.

Wang, W., & Cao, J. (2006). LMI-based criteria for globally robust stability of delayed Cohen-Grossberg neural networks. *IEE Proceedings-Control Theory & Applications*, *153*(4), 397–402.

Wang, X. F., Zhong, G.-Q., Tang, K.-S., Man, K. F., & Liu, Z.-F. (2001). Generating chaos in Chua's circuit via time-delay feedback. *IEEE Transactions on Circuits and Systems I: Fundamental Theory and Application*, *48*(9), 1151–1156.

Xiang, J., Li, Y., & Wei, W. (2007). An improved condition for master–slave synchronization of Lur'e systems with time delay. *Physics Letters A*, *362*(2–3), 154–158.

Yang, X.-S., & Yuan, Q. (2005). Chaos and transient chaos in simple Hopfield neural networks. *Neurocomputing*, *69*(1–3), 232–241.

Yu, H., & Peng, J. (2006). Chaotic synchronization and control in nonlinear-coupled Hindmarsh-Rose neural systems. *Chaos, Solitons and Fractals*, *29*(2), 342–348.

Zhou, J., Chen, T., & Xiang, L. (2006). Robust synchronization of delayed neural networks based on adaptive control and parameters identification. *Chaos, Solitons and Fractals*, *27*(4), 905–913.

Zou, F., & Nossek, J. A. (1993). Bifurcation and chaos in cellular neural networks. *IEEE Transactions on Circuits and Systems I: Fundamental Theory and Application*, *40*(3), 166–173.